Polymorphic ROYalty: The 14th ROY Polymorph Discovered via High-Throughput Crystallization

Jake Weatherston,[a] Michael R. Probert*[a] and Michael J. Hall*[a]

[a]Chemistry, School of Natural and Environmental Sciences, Newcastle University, Newcastle upon Tyne, UK.

ROY, polymorphs, crystallization, ENaCt, high-throughput, single crystal X-ray diffraction, SCXRD, automation.

ABSTRACT: Polymorphism, when a substance can exist in more than one crystalline form yet return to the same liquid or solution phase, is characterized by differences in packing or molecular conformation. Polymorphs often exhibit differing physical properties, and they are therefore particularly important in the development of materials and pharmaceuticals. However, gaining a thorough understanding of the solid-state landscape of a molecule requires exhaustive experimental screening of crystallization conditions, a particular challenge when using classical crystallization methods. We show that high-throughput Encapsulated Nanodroplet Crystallization (ENaCt) can enable the rapid and efficient exploration of the solid-state landscape of highly polymorphic molecules, through an in-depth study of 5-methyl-2-((2-nitrophenyl)amino)thiophene-3-carbonitrile (ROY), the most polymorphic small molecule known. An ENaCt screen encompassing 1,536 individual crystallization experiments, spanning 320 unique conditions, resulted in direct access to single crystals, suitable for X-ray diffraction analysis, for all six of the known polymorphs accessible from solution (Y, R, YN, ON, ORP and R18). In addition, two polymorphs (Y04 and Y19) previously accessed only via melt and heteroseeded melt experiments, and a new polymorph of ROY (O22), the fourteenth to be discovered, were obtained. Furthermore, ENaCt screening resulted in the identification of the first ROY solvate (ROY•methyl anthranilate) and the first example of a ROY dimer, formed via *in situ* oxidation. ENaCt is thus shown to be an impactful tool for the experimental mapping of the solid-state landscape of highly polymorphic molecules and, through the discovery of a new polymorph O22, has ensured that tetradecamorphic ROY retains the world record for most polymorphic small molecule.

Introduction

Polymorphism occurs when a substance exists in multiple accessible crystalline forms. These differ only through the packing arrangement of atoms or molecules, or the molecular conformations within a crystal.[1-4] Polymorphs can have different physical properties, such as stability, hygroscopicity, melting point, hardness, dissolution rate, and even interaction with light (giving rise to color).[5] Polymorphism is of particular importance in the formulation of small molecule drugs, where different polymorphic forms can influence the bioavailability of the compound. Although polymorphism is relatively common, with approximately 4% of small organic molecules having reported polymorphs,[6] there are few examples of highly polymorphic molecules known. These are defined as having nine or more characterized polymorphs such as aripiprazole,[7] flufenamic acid,[8] tolfenamic acid[9], galunisertib[10] and nicotinamide.[11] These highly polymorphic molecules often share common structural features, known as a "polymorphophore", which may offer some explanation to their structural variety.[12,13] The small organic molecule with the highest number of known polymorphs is the olanzapine precursor 5-methyl-2-((2-nitrophenyl)amino)thiophene-3-carbonitrile (Figure 1), also known as ROY due to the red, orange and yellow color of its crystals.[14] ROY is the focus of the study presented herein.

Prior to this work, 13 polymorphs of ROY have been identified, 12 of which have reported structures obtained by single crystal X-ray diffraction: Y,[15] ON,[15] R,[15] OP,[16] YN,[16] ORP,[16] YT04,[17] Y04,[17,18] R05,[19,20] PO13,[21] R18,[22] and Y19,[23] named for their color (yellow (Y), orange (O), red (R), orange red (OR) and pumpkin orange (PO)), morphology (needle (N), plate (P/PL)) and later by year of discovery. RPL has also been identified, but full structural details have yet to be reported.[24,25]

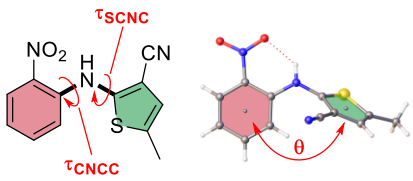

Figure 1. Molecular structure of 5-methyl-2-((2-nitrophenyl)amino)-3-thiophenecabonitrile (ROY). Key descriptors that relate to intramolecular conjugation in ROY highlighted, the phenyl-thiophene rotatable bonds and their associated torsion angles (τ_{SCNC} and τ_{CNCC}) and the phenyl-thiophene mean plane angle (θ, illustrated with the Y polymorph).

Recent crystal structure prediction (CSP) studies indicate that all of the 13 previously known ROY polymorphs exist within 6.6 kJ/mol window of calculated lattice energies, from the most stable polymorph Y to the least stable Y19, with a further 59 predicted Z' = 1 polymorphs lying within this energy range.[26] Thus, despite the considerable research efforts expended by multiple research groups over >25 years in exploring the crystallization of ROY, CSP suggests that many new polymorphs may yet remain to be discovered.

However, the discovery of new ROY polymorphs would require an exhaustive exploration of crystallization space in combination with methods to kinetically trap accessible higher energy forms, beyond the capacity of current approaches. In recent years we have developed the Encapsulated Nanodroplet Crystallization (ENaCt) technology to facilitate crystallization screening for small organic molecules.[22] ENaCt takes advantage of the capabilities of modern liquid-handling robotics, to rapidly setup individual crystallization experiments using nanolitre scale droplets of organic solvent encapsulated within inert oils in a 96-well plate format. Oil encapsulation helps to mediate the rate of solvent loss from the droplets, allowing for slow concentration of the sample and ultimately the growth of single crystals suitable for direct X-ray diffraction (SC-XRD) analysis. ENaCt has, to date, been applied to the crystallization of a wide range of molecular systems including hypocrellin natural products,[27] bicyclic triazolium salts,[28] SARS-CoV-2 protease inhibitors,[29] cannabidiol polymorphs,[30] and flexible hydrogen-bonded organic frameworks (HOFs).[31]

High-throughput methods have previously been applied to the investigation of polymorphism in ROY, including high density polymer-induced heteronucleation (PIHn),[32] and more classical robot-assisted thermal cycling from solution, coupled with RAMAN or PXRD analysis.[33] However, to date such methods have not yielded new crystalline forms of ROY, despite considerable experimental space exploration. We hypothesized that the nanoscale crystallization droplets used in ENaCt would limit the total number of nucleation sites in each individual experimental well, in line with nanoscale confinement methods,[34-36] increasing the chances of trapping new metastable (higher energy) polymorphs. Based on this we examined the solid-state landscape of ROY via ENaCt in the quest for new polymorphs, resulting in three new crystalline forms, including a new 14th polymorph.

High-Throughput Polymorph Screening by ENaCt

A high-throughput (HTP) ENaCt crystallization screen was implemented utilizing 32 solvents with and without water, in combination with 4 encapsulating oils and a "no oil" control. Water as an anti-solvent was included as an experimental variable, as previous observations have shown that the metastable R18 polymorph grew preferentially from organic solvent/water mixtures.[21] Since nucleation is a stochastic process, experimental replicates were also included (5 for each solvent/water/oil combination and 4 for each solvent/water/"no oil" control), resulting in 1,536 individual ENaCt experiments covering 320 different experimental crystallization conditions, utilizing sixteen 96-well plates (see details in SI).

For each chosen solvent, a near saturated stock solution was prepared by portion wise addition of the minimum solvent required to dissolve approximately ~1 mg of ROY. Using an SPT Labtech Mosquito liquid handling robot, 100 nL droplets of these stock solutions were dispensed across 96-well LCP glass plates (100 μm spacer) into pre-dispensed 300 nL oil droplets, or empty wells for "no oil" controls. In parallel, a second set of ENaCt experiments were prepared in which 100 nL ROY stock solutions and 25 nL of water were sequentially taken up by the liquid handling robot, prior to dispensing the mixed sample into 300 nL pre-dispensed oil droplets. The 96-well plates were then sealed with a glass cover slip and monitored using cross-polarized and visible light microscopy over 7 days for the appearance of crystals, with outcomes ranked by apparent crystallinity.

Due to the large number of crystallization experiments undertaken, initial analysis was undertaken using optical microscopy observation of color and morphology. This allowed the categorization of wells as containing crystalline material suitable for SC-XRD analysis and assignment of crystal form. Thus 932 wells were identified as containing single crystals, with 1023 occurrences of specific crystal forms. Following which, a representative selection of crystals was examined by SC-XRD. The crystal form assignment was validated by unit cell

measurements for 310 wells, with full structure solution undertaken for each different form detected. This resulted in the identification by SC-XRD of eleven ROY related crystals, including nine different ROY polymorphs consisting of eight known forms (Figure 2) and one previously unreported polymorph (O22), a ROY dimer and a ROY solvate.

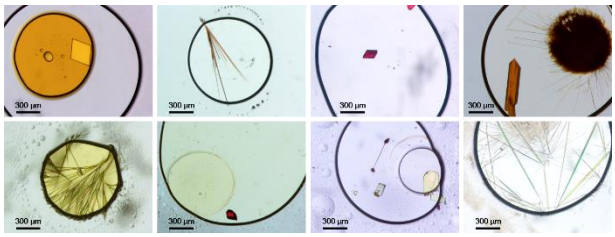

Figure 2. Optical microscopy of ROY crystals from ENaCt polymorph screen (Top left to bottom right: Y, ON, R, ORP, YN, R18, Y04, Y19).

Of the eight known polymorphs obtained from ENaCt screening, five had been previously observed from classical solution-phase crystallization (Y, ON, R, ORP, YN), along with one that was previously discovered using ENaCt (R18). Interestingly, two ROY polymorphs were also obtained that had previously only been accessed via melt microdroplet crystallization (Y04) or hetero-seeded melt crystallization (Y19).[17,22] The observation of "melt-only" polymorphs supports the proposal that metastable forms, beyond those accessible to classical solution phase approaches, can be accessed through ENaCt methods.

Only four of the known polymorphs eluded our screening, none of which are known to crystallize from solution, two of which were discovered from melts (OP, PO13), one from cross-nucleated melts (R05), and one formed via sublimation onto the (010) surface of succinic acid crystals (RPL) for which no SC-XRD data has been previously reported, but for which structures have been proposed.[24,25]

14th ROY polymorph O22

Excitingly, a new orange polymorph of ROY was discovered from a solution of ROY in dimethyl sulfoxide (50 mg/mL ROY in DMSO/mineral oil), herein named O22 (orange 2022). O22 was only observed in a single experimental well, where five discrete orange crystals with a block morphology were formed, all of which gave the same unit cell dimensions determined from SC-XRD. The complete structure of O22 was established, showing that it had crystallized in the monoclinic $P2_1/c$ space group, with Z' = 1 (Figure 3).

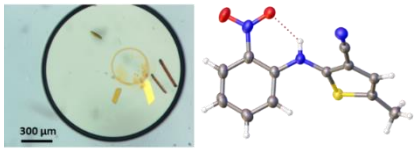

Space Group = $P2_1/c$			
a (Å) =	8.0874(5)	α =	90 °
b (Å) =	19.6111(13)	β =	114.455(2) °
c (Å) =	8.1701(6)	γ =	90 °
τ_{SCNC} =	57.0(2) °	τ_{CNCC} =	5.3(3) °
θ =	56.17(7) °		

Figure 3. Optical microscopy of O22 crystals observed from ENaCt polymorph screen (50 mg/mL ROY in DMSO/mineral oil), crystal structure of O22 (anisotropic displacement parameters shown at 50%), and selected crystal structure parameters.

Like many of the ROY polymorphs, O22 shows an intramolecular H-bond between the arylnitro and diarylamine groups, which flattens the molecule as seen in the small τ_{CNCC} torsion angle (-5.3(3)°). O22 also contains head-to-tail dimers, in which two molecules of ROY are related via an inversion center, resulting in intermolecular nitrile-to-nitrile π-π interactions and diarylamine to nitrile hydrogen bonds. Furthermore, both phenyl-phenyl and thiophene-thiophene π-π stacking interactions can be observed in the [001] and [100] directions respectively (see SI).

In ROY polymorphs, the observed crystal color often correlates with the extent of conjugation between the two ring systems. The SCNS torsional angle (τ_{SCNC}) and the mean plane angle (θ) are often used to estimate the

extent of conjugation, and thus to map to polymorph color.[14,37] In O22, τ_{CNCS} = 57.0(2)° and θ = 56.17(7)°, and thus are consistent with the other known orange polymorphs (see SI).

Interestingly, the structure of O22 appeared to closely match that of a previously predicated polymorph, disclosed by the group of Beran (reported as "Structure Rank #24").[26] The packing similarity between Structure Rank #24 and O22 was assessed using the Crystal Packing Similarity feature within Mercury 4.0, based on the COMPACK geometry analyses of molecular clusters.[38,39] A 15-molecule cluster of both structures was calculated using the default tolerance values (20 % for distances between overlaid molecules and 20 degrees for angles between overlaid molecules). Successful overlay of all 15 molecules with a root-mean-square deviation (RMSD) of 0.137 Å, demonstrated an excellent match between the predicted and experimental structures, supporting the assignment of CSP Structure Rank #24 as polymorph O22 (further supported by related CrystalCMP calculations, see SI).[39] Mapping onto Beran's original CSP study, this suggests that O22 has a lattice energy 4.371 kJ/mol higher than polymorph Y.[26] Thus, O22 sits within the window of lattice energies defined by the other 13 experimentally reported forms, slightly above ORP (E_{rel} = 4.290 kJ/mol) and below R18 (E_{rel} = 4.860 kJ/mol) (see SI).

With the discovery of O22 as the fourteenth reported polymorph, ROY becomes the first known tetradecamorphic system and retains the world record for the most polymorphic small molecule known.

ROY dimer

The ENaCt screen also revealed a single experimental well containing a yellow plate-like crystal (14 mg/mL ROY in 2-nitroethanol/mineral oil), with no other crystals observed from the use of 2-nitroethanol as the solvent. Analysis by SC-XRD revealed that the crystal did not contain ROY itself, but the *meso*-diastereomer of a molecule formed via an oxidative dimerization of ROY (figure 4).

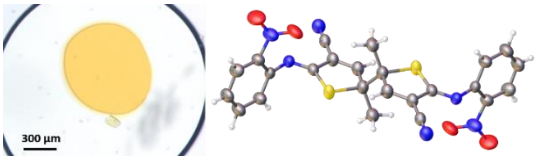

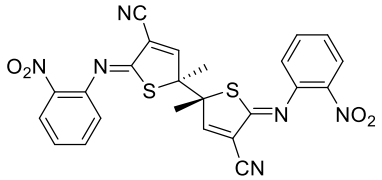

Space Group = *C*2/*c*			
a (Å) =	15.1969(4)	α =	90 °
b (Å) =	7.7513(2)	β =	92.640(1) °
c (Å) =	19.9721(5)	γ =	90 °

Figure 4: Optical microscopy of ROY dimer crystal observed from ENaCt polymorph screen (14.3 mg/L ROY in 2-nitroethanol/mineral oil), crystal structure of ROY dimer (anisotropic displacement parameters shown at 50%, disordered nitro groups displayed as the major disorder component for clarity), molecular structure and selected crystal structure parameters.

This ROY dimer had crystallized in the monoclinic C2/c space group with a Z' = 0.5, with the molecule containing an inversion center. The ROY dimer shows significant structural changes from the known ROY polymorphs. In particular, the transformation of a bridging amine to an imine results in the extended planarization of the newly formed sulfur heterocycle (τ_{SCNC} = 7.8(6)°), with concurrent loss of the nitro to amine intramolecular S(6) H-bond (τ_{CNCC} = 75.6(5)°).

We postulated that the observed ROY dimer was likely formed during the crystallization experiment, as no evidence of the dimer can be observed by NMR or HRMS of the initial ROY samples (see SI). We propose that due to poor crystallization of ROY from 2-nitroethanol, the sample remains in solution for a sufficiently long time for an oxidative coupling to occur, likely mediated by atmospheric oxygen. The highly crystalline ROY dimer then preferentially crystallizes from solution.

Methyl anthranilate solvate of ROY

Additionally, during the ENaCt polymorph screen, orange needle-like crystals were observed to grow from methyl anthranilate (50 mg/mL of ROY in methyl anthranilate) in all four encapsulating oils, that did not match known forms of ROY through either morphology/color, or via unit cell analysis. Only weak diffraction

was obtained, however this was sufficient to obtain both space group ($P2_1/c$) and unit cell parameters. Interestingly, the new form showed similarities to Y19, but with an elongation of the c axis (12.5 Å to 14.3 Å). To obtain higher quality crystals a follow up seeded ENaCt experiment was undertaken in which the original needle-like crystals were harvested, pooled and crushed to generate a microcrystalline seed stock. Seed material was then suspended in mineral oil, and this "seeded" mineral oil was used as the encapsulating material for the next set of ENaCt experiments (96 well plate, 50 mg/mL ROY in methyl anthranilate, mineral oil).[30] This resulted in rapid growth of the target crystal form, only one day elapsing before all 96 wells contained orange needle-like crystals, with significantly improved crystal volume and quality, resulting in successful structure solution by SC-XRD (Figure 5).

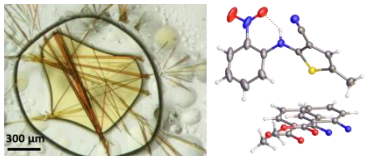

Space Group = $P2_1/c$			
a (Å) =	3.88127(11)	α =	90 °
b (Å) =	23.7098(7)	β =	93.145(3) °
c (Å) =	14.3056(3)	γ =	90 °
τ_{SCNC} =	53.2(3) °	τ_{CNCC} =	8.7(4) °
θ =	124.78(9) °		

Figure 5. Optical microscopy of ROY:methyl anthranilate observed from seeded ENaCt experiments (50 mg/mL ROY in methyl anthranilate/mineral oil(seeded)), crystal structure of ROY:methyl anthranilate (anisotropic displacement parameters shown at 50%, disordered solvent modelled over two positions as shown), and selected crystal structure parameters.

SC-XRD showed that ROY had crystallized with methyl anthranilate to form a non-stoichiometric channel solvate, with a solvent occupancy of 0.220(3) per ROY molecule. Within the ROY:methyl anthranilate solvate, ROY showed a packing motif with high similarity to Y19 (supported by similarity comparison score of 3.06 using CrystalCMP, see SI).[40]

The major structural differences from Y19 was the presence of an increased spacing between adjacent ROY molecules in the crystallographic [100] direction, creating a void. Channels of residual electron density running down the [001] direction in this void space were modelled as disordered methyl anthranilate extending in a continuum down the channels (see SI). Although the occurrence of solvates of small organic molecules is common, ROY:methyl anthranilate is the first reported solvate known for the highly studied ROY system.

Impact of ENaCt on Polymorph Propensity

To better understand the ability of ENaCt to access different polymorphs, the propensity of polymorph occurrence was examined the whole polymorph screen. From 1,536 individual crystallisation experiments, 932 wells contained 1023 occurrences of identifiable ROY crystal forms, with 843 containing a single crystal form, and 89 wells exhibiting concomitant crystallisation of more than one crystal form (87 wells containing two different polymorphs, and 2 wells containing three different polymorphs) (Figure 6, and SI).

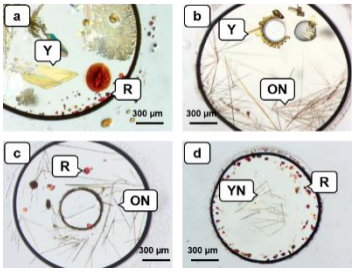

Figure 6. Optical microscopy of concomitant crystallization of ROY polymorphs, from ENaCt screen. (a) Y and R, (b) Y and ON, (c) R and ON, (d) R and YN.

Of the 1,023 wells containing of identifiable ROY single crystal forms, 1,016 were ROY polymorphs with 7 occurrences of the ROY dimer and ROY solvate forms. ON was the most commonly observed with 404 wells containing ON crystals, 26.3% of the total. The most thermodynamically stable Y polymorph was second (369,

24.0%), followed by YN (114, 7.4%) and R (93, 6.1%) which together made up the majority of the polymorphs observed, R18 (17, 1.1%), Y04 (9, 0.6%), Y19 (5, 0.3%), ORP (3, 0.2%) and O22 (1, 0.1%) being somewhat rarer. ON and YN are kinetically favoured polymorphs, whilst the thermodynamically most stable Y is typically formed under equilibrium conditions.[16] Thus, the observation of ON and YN as major polymorphs in ENaCt further supports the hypothesis that this approach can successful trap high relative energy kinetic polymorphs. The ENaCt experiments which included water as an anti-solvent showed an increase in the presence of higher energy metastable forms, YN increasing by 59% (44 occurrences in 768 ENaCt experiments without water → 70 in 768 ENaCt experiments with water), R18 by 83% (6 → 11), whilst ORP (0 → 3) and Y19 (0 → 5), the highest energy polymorph, were only observed when water was present.[35] In these cases it is likely that the presence of an anti-solvent in the ENaCt droplet, speeds crystallisation and aids in the kinetic trapping of metastable polymorphs.

Conclusions

Our investigation of the ROY polymorph landscape has spanned 1,536 individual crystallisation experiments, including 320 unique crystallisation conditions. This has resulted in access to eight known ROY polymorphs (Y, ON, YN, R, ORP, Y04, Y19 and R18), including two metastable crystal forms that were previously considered inaccessible to solution phase crystallisation (Y04 and Y19). In addition, ENaCt screening has revealed a novel ROY solvate, an unexpected ROY dimer, and the fourteenth discovered polymorph (O22). High-throughput encapsulated nanodroplet crystallisation (ENaCt) is thus shown to be a powerful tool for exploring the solid-state landscape of a small molecule, particularly through the formation and trapping of high energy metastable polymorphs, including "melt-only" forms. Further studies to better understand the mechanism of metastable polymorph trapping in ENaCt will form the focus of future work.

ASSOCIATED CONTENT

Supporting Information. Experimental information, including ENaCt and classical crystallization procedures and outcomes, crystallographic data tables, packing similarity analysis, and further structural discussion of new ROY forms. CCDC 2381874-2381884 contains the supplementary crystallographic data for this paper. This material is available free of charge via the Internet at http://pubs.acs.org, or from The Cambridge Crystallographic Data Centre via www.ccdc.cam.ac.uk/structures.

AUTHOR INFORMATION

Corresponding Authors

* michael.probert@newcastle.ac.uk
* michael.hall@newcastle.ac.uk

Author Contributions

The manuscript was written through contributions of all authors. JW carried out crystallization experiments, SC-XRD analysis, and produced the draft manuscript. MRP and MJH provided supervision and advice. MRP assisted with SC-XRD analysis. MJH and MRP produced the final manuscript. All authors have given approval for the final version of the manuscript.

ACKNOWLEDGMENT

The following funding is acknowledged: Engineering and Physical Sciences Research Council (EP/W02098X/1; EP/W021129/1) and (JW) Indicatrix Crystallography Ltd. EPSRC UK National Mass Spectrometry Facility at Swansea University is acknowledged for analytical support. Dr Sarah Heaps (Durham University, UK) is also acknowledged for additional supervision support for JW.

REFERENCES

1. J. P. Brog, C. L. Chanez, A. Crochet and K. M. Fromm, Polymorphism, what it is and how to identify it: a systematic review. *RSC Adv.*, 2013, **3**, 16905–16931. DOI: 10.1039/C3RA41559G

2. A. J. Cruz-Cabeza and J. Bernstein, Conformational Polymorphism. *Chem. Rev.*, 2014, **114**, 2170–2191. DOI: 10.1021/cr4002449d

3. A. J. Cruz-Cabeza, S. M. Reutzel-Edens and J. Bernstein, Facts and fictions about polymorphism. *Chem. Soc. Rev.*, 2015, **44**, 8619–8635. DOI: 10.1039/C5CS00227C

4. A. J. Cruz-Cabeza, N. Feeder and R. J. Davey, Open questions in organic crystal polymorphism. *Commun. Chem.*, 2020, **3**, 142. DOI: 10.1038/s42004-020-00388-9

5. B. A. Nogueira, C. Castiglioni and R. Fausto, Color polymorphism in organic crystals. *Commun. Chem.*, 2020, **3**, 34. DOI: 10.1038/s42004-020-0279-0

6. K. Kersten, R. Kaur and A. Matzger, Survey and analysis of crystal polymorphism in organic structures. *IUCrJ,* 2018, **5**, 124–129. DOI: 10.1107/S2052252518000660

7. T. A. Zeidan, J. T. Trotta, P. A. Tilak, M. A. Oliveira, R. A. Chiarella,B. M. Foxman, Ö. Almarsson and M. B. Hickey, An unprecedented case of dodecamorphism: the twelfth polymorph of aripiprazole formed by seeding with its active metabolite. *CrystEngComm.*, 2016, **18**, 1486–1488. DOI: 10.1039/C5CE02467F

8. V. López-Mejías, J. W. Kampf and A. J. Matzger, Nonamorphism in Flufenamic Acid and a New Record for a Polymorphic Compound with Solved Structures. *J. Am. Chem. Soc.*, 2012, **134**, 9872–9875. DOI: 10.1021/ja302601f

9. P. Sacchi, S. M. Reutzel-Edens and A. J. Cruz-Cabeza, The unexpected discovery of the ninth polymorph of tolfenamic acid. *CrystEngComm.*, 2021, **23**, 3636–3647. DOI: 10.1039/D1CE00343G

10. R. M. Bhardwaj, J. A. McMahon, J. Nyman, L. S. Price, S. Konar, I. D. H. Oswald, C. R. Pulham, S. L. Price and S. M. Reutzel-Edens, A Prolific Solvate Former, Galunisertib, under the Pressure of Crystal Structure Prediction, Produces Ten Diverse Polymorphs. *J. Am. Chem. Soc.*, 2019, **141**, 13887–13897. DOI: 10.1021/jacs.9b06634

11. X. Li, X. Ou, B. Wang, H. Rong, B. Wang, C. Chang, B. Shi, L. Yu, M. Lu, Rich polymorphism in nicotinamide revealed by melt crystallization and crystal structure prediction. *Commun. Chem.*, 2020, **3**, 152. DOI: 10.1038/s42004-020-00401-1

12. K. M. Lutker, Z. P. Tolstyka and A. J. Matzger, Investigation of a Privileged Polymorphic Motif: A Dimeric ROY Derivative. *Cryst. Growth Des.*, 2008, **8**, 136–139. DOI: 10.1021/cg700921w

13. O. G. Uzoh , A. J. Cruz-Cabeza and S. L. Price, Is the Fenamate Group a Polymorphophore? Contrasting the Crystal Energy Landscapes of Fenamic and Tolfenamic Acids. *Cryst. Growth Des.*, 2012, **12** , 4230—4239. DOI: 10.1021/cg3007348

14. L. R. Warren, E. McGowan, M. Renton, C. A. Morrison and N. P. Funnell, Direct evidence for distinct colour origins in ROY polymorphs. *Chem. Sci.*, 2021, **12**, 12711–12718. DOI: 10.1039/D1SC04051K

15. G. A. Stephenson, T. B. Borchardt, S. R. Byrn, J. Bowyer, C. A. Bunnell, S. V. Snorek and L. Yu, Conformational and color polymorphism of 5-methyl-2-[(2-nitrophenyl) amino]-3-thiophenecarbonitrile. *J. Pharm. Sci.*, 1995, **84**, 1385–1386. DOI: 10.1002/jps.2600841122

16. L. Yu, G. A. Stephenson, C. A. Mitchell, C. A. Bunnell, S. V. Snorek, J. J. Bowyer, T. B. Borchardt, J. G. Stowell and S. R. Byrn, Thermochemistry and Conformational Polymorphism of a Hexamorphic Crystal System. *J. Am. Chem. Soc.*, 2000, **122**, 585–591. DOI: 10.1021/ja9930622

17. S. Chen, I. A. Guzei and L. Yu, New Polymorphs of ROY and New Record for Coexisting Polymorphs of Solved Structures. *J. Am. Chem. Soc.*, 2005, **127**, 9881–9885. DOI: 10.1021/ja052098t

18. X. Li , X. Ou , H. Rong , S. Huang , J. Nyman , L. Yu and M. Lu, The Twelfth Solved Structure of ROY: Single Crystals of Y04 Grown from Melt Microdroplets. *Cryst. Growth Des.*, 2020, **20**, 7093—7097. DOI: 10.1021/acs.cgd.0c01017

19. S. Chen, H. Xi and L. Yu, Cross-Nucleation between ROY Polymorphs. *J. Am. Chem. Soc.*, 2005, **127**, 17439–17444. DOI: 10.1021/ja056072d

20. M. Tan, A. Shtukenberg, W. Xu, E. Dooryhee, S. Nichols, M. Ward, B Kahr and Q. Zhu, ROY revisited, again: the eighth solved structure. *Faraday Discuss.*, 2018, **211**, 477–491. DOI: 10.1039/C8FD00039E

21. S. Gushurst, J. Nyman and S. X. M. Boerrigter, The PO13 crystal structure of ROY. *CrystEngComm*, 2019, **21**, 1363–1368. DOI: 10.1039/C8CE01930D

22. A. R. M. Tyler, R. Ragbirsingh, C. J. McMonagle, P. G. Waddell, S. E. Heaps, J. W. Steed, P. Thaw, M. J. Hall and M. R. Probert, Encapsulated Nanodroplet Crystallization of Organic-Soluble Small Molecules. *Chem*, 2020, **6**, 1755–1765. DOI: 10.1016/j.chempr.2020.04.009

23. A. Lévesque, T. Maris and J. D. Wuest, ROY Reclaims Its Crown: New Ways To Increase Polymorphic Diversity. *J. Am. Chem. Soc.*, 2020, **142**, 11873–11883. DOI: 10.1021/jacs.0c04434

24. C. Mitchell, L. Yu and M. Ward, Selective Nucleation and Discovery of Organic Polymorphs through Epitaxy with Single Crystal Substrates. *J. Am. Chem. Soc.*, 2001, **123**, 10830–10839. DOI: 10.1021/ja004085f

25. J. Nyman, L. Yu and S. M. Reutzel-Edens, Accuracy and reproducibility in crystal structure prediction: the curious case of ROY. *CrystEngComm*, 2019, **21**, 2080–2088. DOI: 10.1039/C8CE01902A

26. G. J. O. Beran, I. J. Sugden, C. Greenwell, D. H. Bowskill, C. C. Pantelides and C. S. Adjiman, How many more polymorphs of ROY remain undiscovered. *Chem. Sci.*, 2022, **13**, 1288–1297. DOI: 10.1039/D1SC06074K

27. Z. Y. AlSubeh, A. Waldbusser, H. A. Raja, C. J. Pearce, K. L. Ho, M. J. Hall, M. R. Probert, N. H. Oberlies and S. Hematian, Structural Diversity of Perylenequinones Is Driven by Their Redox Behavior. *J. Org. Chem.*, 2022, **87**, 2697—2710. DOI: 10.1021/acs.joc.1c02639

28. J. Zhu, I. Moreno, P. Quinn, D. S. Yufit, L. Song, C. M. Young, Z. Duan, A. R. Tyler, P. G. Waddell, M. J. Hall, M. R. Probert, A. D. Smith and A. C. O'Donoghue, The Role of the Fused Ring in Bicyclic Triazolium Organocatalysts: Kinetic, X-ray, and DFT Insights. *J. Org. Chem.*, 2022, **87**, 4241—4253. DOI: 10.1021/acs.joc.1c03073

29. M. S. Cooper, L. Zhang, M. Ibrahim, K. Zhang, X. Sun, J. Röske, M. Göhl, M. Brönstrup, J. K. Cowell, L. Sauerhering, S. Becker, L. Vangeel, D. Jochmans, J. Neyts, K. Rox, G. P. Marsh, H. J. Maple and R. Hilgenfeld, Diastereomeric Resolution Yields Highly Potent Inhibitor of SARS-CoV-2 Main Protease. *J. Med. Chem.*, 2022, **65**, 13328—13342. DOI: 10.1021/acs.jmedchem.2c01131

30. H. E. Straker, L. McMillan, L. Mardiana, G. R. Hebberd, E. Watson, P. G. Waddell, M. R. Probert and M. J. Hall, Polymorph prediction through observed structural isomorphism leading to a new crystalline form of cannabidiol. *CrystEngComm*, 2023, **25**, 2479—2484. DOI: 10.1039/D3CE00041A

31. Q. Zhu, L. Wei, C. Zhao, H. Qu, B. Liu, T. Fellowes, S. Yang, A. Longcake, M. J. Hall, M. R. Probert, Y. Zhao, A. I. Cooper and M. A. Little, Soft Hydrogen-Bonded Organic Frameworks Constructed Using a Flexible Organic Cage Hinge. *J. Am. Chem. Soc.*, 2023, **145**, 23352–23360. DOI: 10.1021/jacs.3c09246

32. L. Y. Pfund, A. J. Matzger, Towards Exhaustive and Automated High-Throughput Screening for Crystalline Polymorphs. *ACS Comb. Sci.*, 2014, **16**, 309-313. DOI: 10.1021/co5000434

33. V. W. Rosso, Z. Yin, H. Abourahma, A. Furman, S. Sharif, A. Werneth, J. M. Stevens, F. Roberts, D. Aulakh, R. Sommer and A. A. Sarjeant, High-Throughput Crystallization Screening Technique with Transmission PXRD Analysis. *Org. Process Res. Dev.*, 2023, **27**, 1437—1444. DOI: 10.1021/acs.oprd.3c00091

34. Q. Jiang and M. D. Ward, Crystallization under nanoscale confinement. *Chem. Soc. Rev.*, 2014, **43**, 2066—2079. DOI: 10.1039/C3CS60234F

35. J. L. Hilden, C. E. Reyes, M. J. Kelm, J. S. Tan, J. G. Stowell and K. R. Morris, Capillary Precipitation of a Highly Polymorphic Organic Compound, *Cryst. Growth Des.*, 2003, **3**, 921–926. DOI: 10.1021/cg034061v

35. I. Ziemecka, S. Gokalp, S. Stroobants, F. Brau, D. Maes and A. De Wit, Polymorph Selection of ROY by Flow-Driven Crystallization. *Crystals*, 2019, **9**, 351. DOI: 10.3390/cryst9070351

36. F. C. Meldrum and C. O'Shaughnessy, Crystallization in Confinement, *Adv. Mater.*, 2020, **32**, 2001068-2001068. DOI: 10.1002/adma.202001068

37. X. Feng, A. D. Beckea and E. R. Johnson, Theoretical investigation of polymorph- and coformer-dependent photoluminescence in molecular crystals. *CrystEngComm*, 2021, **23**, 4264—4271. DOI: 10.1039/D1CE00383F

38. C. F. Macrae, I. Sovago, S. J. Cottrell, P. T. A. Galek, P. McCabe, E. Pidcock, M. Platings, G. P. Shields, J. S. Stevens, M. Towler and P. A. Wood, Mercury 4.0: from visualization to analysis, design and prediction. *J. Appl. Crystallogr.*, **53**, 2020, 226-235. DOI: 10.1107/S1600576719014092

39. J. A. Chisholm, and S. Motherwell, COMPACK: a program for identifying crystal structure similarity using distances. *J. Appl. Crystallogr.*, **38**, 2005, 228-231. DOI: 10.1107/S0021889804027074

40. J. Rohliček and E. Skořepova, CrystalCMP: automatic comparison of molecular structures. *J. Appl. Crystallogr.*, **53**, 2020, 841-847. DOI: 10.1107/S1600576720003787